Reviews in Mineralogy & Geochemistry
Vol. 68, pp. 31-53, 2008

Nucleosynthesis and Chemical Evolution of Oxygen

Bradley S. Meyer
Department of Physics and Astronomy
Clemson University
Clemson, South Carolina 29634, U.S.A.
mbradle@clemson.edu

Larry R. Nittler and Ann N. Nguyen
Department of Terrestrial Magnetism
Carnegie Institute of Washington
Washington, D.C. 20015, U.S.A.

Scott Messenger
Robert M. Walker Laboratory for Space Science
NASA Johnson Space Center
Houston, Texas 77058, U.S.A.

ABSTRACT

Of the elements strictly synthesized in stars, oxygen is by far the most abundantly produced. We review the nucleosynthesis and galactic chemical evolution of this important element. We then review its isotopic composition in presolar grains recovered from primitive meteorites and from interplanetary dust particles. As we describe, knowledge of these isotopic compositions provide important constraints on theories of nucleosynthesis, stellar evolution, and galactic chemical evolution.

INTRODUCTION

The isotopes of oxygen are crucial diagnostics of nucleosynthesis and galactic chemical evolution. This is due in large part to oxygen's high abundance. It is the third most abundant element in the Galaxy, though considerably less abundant than hydrogen and helium, which are principally produced in primordial nucleosynthesis. Of the elements strictly synthesized in stars, oxygen is by far the most abundantly produced. Oxygen's abundance is nearly equal to that of all the other heavy elements (elements with atomic number greater than that of helium) combined (e.g., Lodders 2003). This high abundance means that it is readily observable in the atmospheres of stars. It also means that oxygen is a dominant player in chemical reactions taking place in stellar outflows, in the interstellar medium, and in the early Solar System.

The abundance of oxygen is dominated by that of ^{16}O, which is the third most abundant isotope in the Galaxy. The other stable isotopes of oxygen are considerably less abundant. ^{18}O is the 25th most abundant isotope in the Solar System, with an abundance about 0.2% that of ^{16}O. ^{17}O is the 34th most abundant isotope in the Solar System, and its abundance is 0.03% that of ^{16}O[1]. Despite the low relative abundances of ^{17}O and ^{18}O, they are still sufficiently abundant that

[1] The isotopic abundances and rankings presented here are those according to the compilation of Lodders (2003). For further details on oxygen abundances in the Solar System, please see Davis et al. (2008). The interested reader may also wish to explore the Solar System abundances and their rankings with the Webnucleo online solar abundances tool available at *http://www.webnucleo.org/home/online_tools/solar_abundances/*

1529-6466/08/0068-0004$05.00 DOI: 10.2138/rmg.2008.68.4

they can be measured in stellar atmospheres. As we shall also see, oxygen isotopic abundances are also readily measured in presolar grains in meteorites and interplanetary dust particles. These measurements provide key constraints on nucleosynthesis and stellar evolution.

Also contributing to oxygen's importance as a diagnostic is the fact that its three stable isotopes are predominantly made in different burning epochs during the life of a star. As we shall see below, ^{17}O is predominantly made in hydrogen burning, ^{18}O is predominantly made in the early stages of helium burning, and ^{16}O is made in the later part of helium burning. Thus, the isotopic composition of a stellar atmosphere or a presolar grain provides clues to the stellar region in which the major part of the material was synthesized.

Finally, a third significant aspect of oxygen's role as a diagnostic of nucleosynthesis and galactic chemical evolution is the primary versus secondary nature of the different isotopes. ^{16}O is a primary isotope, that is, an isotope that can be synthesized in a star initially composed only of hydrogen and helium, while ^{17}O and ^{18}O are secondary isotopes, which means that their formation requires pre-existing seed nuclei from previous stellar generations. As a consequence, the abundance of ^{16}O relative to those of ^{17}O and ^{18}O changed with time in the Galaxy's history. Measurements of oxygen abundances in stars or in presolar grains of different ages can thus provide important clues about the chemical evolution of the Galaxy (e.g., Clayton 1988).

The goal of this paper is to review the nucleosynthesis and chemical evolution of the isotopes of oxygen and the manifestations of these processes in astronomical and cosmochemical samples. We begin in the section "Nucleosynthesis of the Isotopes of Oxygen" with a review of the nucleosynthesis of oxygen isotopes in the different burning stages in stars and follow up with an analysis of the oxygen isotopic abundances from high-mass and low-mass stars. We then turn in the section "Chemical Evolution of the Isotopes of Oxygen" to a review of the key issues of the galactic chemical evolution of the oxygen isotopes. In the section "Oxygen in Presolar Grains," we review some of the implications of oxygen data on presolar grains for nucleosynthesis and chemical evolution. In the last section, we present some concluding remarks.

NUCLEOSYNTHESIS OF THE ISOTOPES OF OXYGEN

As a whole, our Universe has only about 10^{-10} nucleons for every photon. By contrast, the corresponding number in stars is close to unity. The low nucleon-to-photon ratio in the early Universe strongly inhibited build-up of heavy nuclei, and, as a consequence, primordial nucleosynthesis did not produce any oxygen. The oxygen present in our Solar System was thus made in stars. In this section, we first review oxygen nucleosynthesis in the main stellar burning stages. We then analyze the oxygen yields predicted for high-mass and low-mass stars, as well as for novae and Type Ia supernovae.

Production of oxygen in mainline stellar burning stages

Hydrogen burning. Stars shine. As a consequence, they radiate away energy. To compensate this energy loss and maintain their pressure support against gravitational contraction, stars convert nuclear energy into thermal energy by fusing lighter nuclei into heavier ones. This nuclear burning proceeds through a series of stages in which the ashes of one stage serve as the fuel for the next. This sequence of burning stages progresses until either electron degeneracy replaces thermal pressure to support the star or the star burns the nuclei all the way to iron, from which no more nuclear energy can be extracted by fusion.

The first nuclear fuel available to stars is hydrogen, which stars burn into ^{4}He. Stars with the mass of the Sun or less burn hydrogen at relatively low temperatures (10-20 million K) via the so-called PP chains. Because the PP chains only involve isotopes of hydrogen, helium, lithium, and beryllium, these reaction chains do not affect the stellar abundance of oxygen. In contrast,

stars more than about 1.2 times the mass of the Sun attain somewhat higher temperatures and can thus burn hydrogen by the more efficient process known as CNO burning. In this process, the production of ^{4}He from ^{1}H is catalyzed by two coupled cycles involving isotopes of carbon, nitrogen, and oxygen. In the CN cycle, the reaction sequence is: $^{12}C + {}^{1}H \rightarrow {}^{13}N + \gamma$ (here γ represents energy released during the reaction as a gamma ray which subsequently deposits its energy locally); $^{13}N \rightarrow {}^{13}C + e^{+} + \nu_e$ (here e^{+} represents a positron and ν_e represents an electron-type neutrino); $^{13}C + {}^{1}H \rightarrow {}^{14}N + \gamma$; $^{14}N + {}^{1}H \rightarrow {}^{15}O + \gamma$; $^{15}O \rightarrow {}^{15}N + e^{+} + \nu_e$; and $^{15}N + {}^{1}H \rightarrow {}^{12}C + {}^{4}He$. This last reaction closes the cycle. Roughly 0.1% of the time, however, ^{15}N does not return to ^{12}C, but rather captures a proton to become ^{16}O: $^{15}N + {}^{1}H \rightarrow {}^{16}O + \gamma$. This initiates the NO cycle: $^{15}N + {}^{1}H \rightarrow {}^{16}O + \gamma$; $^{16}O + {}^{1}H \rightarrow {}^{17}F + \gamma$; $^{17}F \rightarrow {}^{17}O + e^{+} + \nu_e$; and $^{17}O + {}^{1}H \rightarrow {}^{14}N + {}^{4}He$. It is the NO cycle that predominantly involves oxygen isotopes in hydrogen burning, although the minor pathway $^{17}O + {}^{1}H \rightarrow {}^{18}F + \gamma$; $^{18}F \rightarrow {}^{18}O + e^{+} + \nu_e$; and $^{18}O + {}^{1}H \rightarrow {}^{15}N + {}^{4}He$ brings ^{18}O into play as well.

During CNO burning, the slow reaction is $^{14}N + p \rightarrow {}^{15}O + \gamma$ (here p represents a proton; this reaction can also be written as $^{14}N(p,\gamma)^{15}O$). This means that CNO cycling tends to convert the initial abundances of carbon and oxygen into ^{14}N. This is evident in Figure 1, which shows the mass fractions of various species yielded by a hydrogen burning calculation with the Clemson

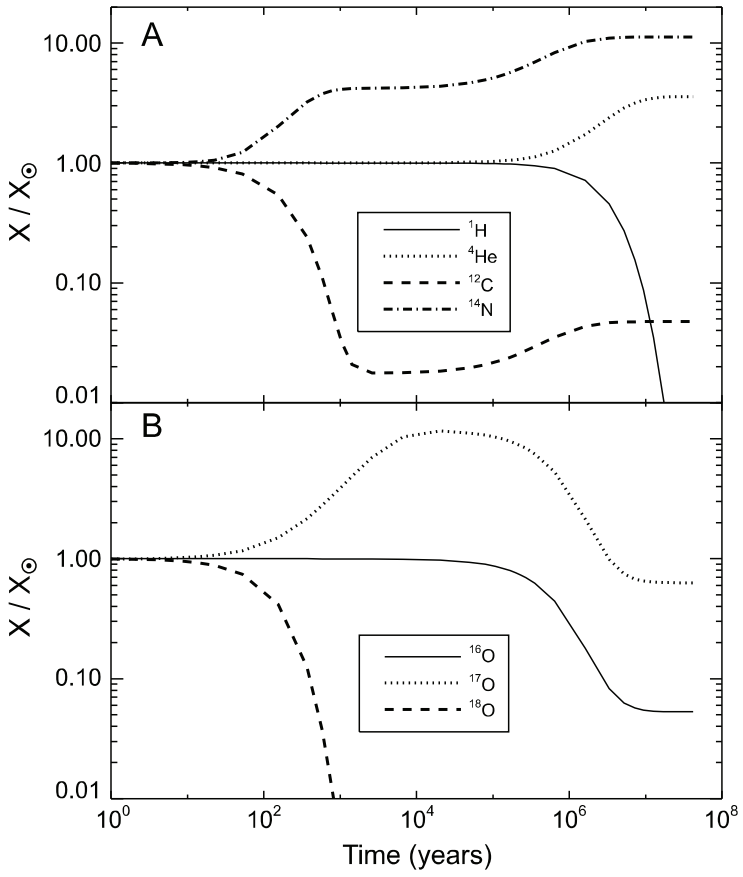

Figure 1. Evolution of the mass fractions of the indicated species during hydrogen burning at a temperature of 3×10^{7} K and 10 g/cm^{3}.

nucleosynthesis network code (Jordan and Meyer 2004). The calculation began with a solar abundance distribution (Anders and Grevesse 1989) and was run at a constant temperature of 3×10^7 K and a density of 10 g/cm^3, conditions fairly typical of hydrogen burning in the cores of massive stars. As is evident, CN burning converts ^{12}C into ^{14}N early in the burning while the reaction $^{18}O + p \rightarrow {}^{15}N + {}^{4}He$ quickly depletes the initial ^{18}O and involves O in the main CNO cycling. As time progresses in the calculation, the ^{17}O abundance rises due to proton capture onto ^{16}O and achieves a maximum enrichment of about a factor of ten relative to its initial abundance. After about 10^4 years, however, the ^{17}O abundance attains a steady state as destruction via $^{17}O(p,{}^{4}He){}^{14}N$ balances the production from ^{16}O. Finally, after 10^6 years, the full CNO bi-cycle achieves a steady state. The ^{1}H converts into ^{4}He and the oxygen isotopes convert into ^{14}N.

After complete CNO burning, ^{4}He and ^{14}N are enriched while ^{12}C and ^{16,17,18}O are all depleted (Fig. 1). Nevertheless, if the CNO cycling is not complete or the burning happens at a lower temperature, the matter may be enriched in ^{17}O and depleted in ^{16,18}O, as is the case in Figure 1B at a time of 10^6 yr. This is typically the case in the envelopes of stars that have experienced dredge up (mixing) of matter from a hydrogen burning shell.

Helium burning. After a star has burned its hydrogen into helium, the next available fuel is the ^{4}He. Due to the lack of stable isotopes with mass number five and eight, the helium burning proceeds via the triple-alpha process, which may be viewed as the reaction $^4He + {}^4He + {}^4He \rightarrow {}^{12}C + \gamma$. Helium burning typically occurs at temperatures of ~1-3$\times10^8$ K and densities near 1000 g/cm^3. Figure 2 shows the evolution of mass fractions relative to solar values in a helium burning calculation at a temperature of 2.5×10^8 K and a density of 1000 g/cm^3 and using as the initial abundances the final yields from the previous hydrogen burning calculation.

In the initial stages of helium burning, the abundant ^{14}N captures ^{4}He to produce ^{18}F, which decays to ^{18}O, thereby strongly enriching ^{18}O relative to ^{16}O and ^{17}O. The ^{18}O itself then captures another ^{4}He, which depletes the ^{18}O and creates ^{22}Ne. At the high temperature of the calculation in Figure 2, this conversion of ^{14}N into ^{22}Ne occurs within the first 0.1 yr. As this is occurring, the triple-alpha reaction is also converting ^{4}He into ^{12}C. Beginning at about one year, the ^{12}C becomes sufficiently abundant that it can capture ^{4}He to become ^{16}O. This strongly enriches ^{16}O relative to the other oxygen isotopes. The ^{12}C/^{16}O ratio resulting from helium burning determines the nature of the subsequent carbon burning in the star, which, in turn, determines the whole subsequent shell structure of the star (e.g., El Eid et al. 2004). For this reason, the reaction $^{12}C(^{4}He,\gamma)^{16}O$, which is not yet fully characterized in the laboratory, is the subject of intense experimental study.

As a final point, it is worth noting that the reaction $^{16}O + {}^4He \rightarrow {}^{20}Ne + \gamma$ does not occur at helium-burning temperatures because of the lack of an appropriate resonance in ^{20}Ne. A dominant mechanism for two nuclei to react is to proceed through formation of a compound nucleus, which is, in effect, a resonance in the scattering state of the two interacting nuclei. The compound nucleus subsequently breaks apart into different nuclei or de-excites to the product nucleus ground state. For example, when ^{12}C and ^{4}He combine, they can form an excited state (that is, a resonance) of ^{16}O if the energy and the spin and parity changes in the interaction are appropriate. Most of the time, the excited ^{16}O nucleus will break apart into ^{4}He and ^{12}C again. In some cases, however, the excited ^{16}O decays by photon emission to the ground state. In the case of ^{20}Ne, the typical interaction energies of ^{16}O and ^{4}He in helium burning are appropriate to form the 4.969 MeV state in ^{20}Ne, which would make an ideal compound nucleus, but the spin and parity changes are not right, so the reaction does not occur (e.g., Clayton 1968). Alpha capture therefore ceases at ^{16}O, and, as a consequence ^{16}O is, in fact, the dominant product of helium burning.

From Figure 2, it is clear that there is a phase in helium burning in which ^{18}O is enhanced while ^{16}O and ^{17}O are depleted. As the burning progresses, however, the ^{18}O converts to ^{22}Ne

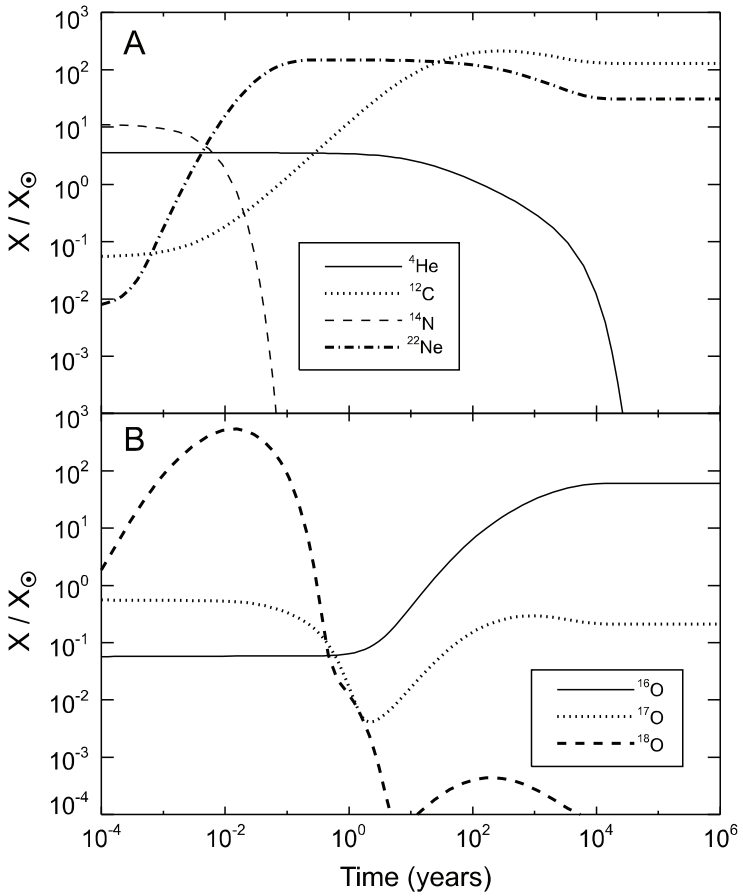

Figure 2. Evolution of the mass fractions of the indicated species during helium burning at a temperature of 2.5×10^8 K and a density of 1.0×10^3 g/cm^3.

and ^{16}O becomes the dominant oxygen isotope. Because the ^{16}O so greatly dominates the other oxygen isotopes after helium burning, we will henceforth neglect these minor isotopes in the subsequent discussion.

Carbon burning. The next stellar burning stage is carbon burning. Carbon burning typically occurs at temperatures near 9×10^8 K and densities near 10^5 g/cm^3. It predominantly converts ^{12}C into ^{20}Ne and ^{24}Mg via the reactions $^{12}C + {}^{12}C \rightarrow {}^{20}Ne + {}^{4}He$ and $^{12}C + {}^{12}C \rightarrow {}^{24}Mg + \gamma$. At carbon-burning temperatures, there are resonances in the $^{16}O(^{4}He,\gamma)^{20}Ne$ reaction available that allow the reaction to proceed efficiently. This means that the ^{16}O left after helium burning is depleted somewhat during carbon burning due to capture of ^{4}He produced by the main carbon-burning reactions.

Neon burning. After carbon burning, a star burns neon. This effectively occurs in a two-step process. The first reaction is $^{20}Ne + \gamma \rightarrow {}^{16}O + {}^{4}He$. This reaction is endothermic. The ^{4}He produced, however, then captures on another ^{20}Ne to produce ^{24}Mg. This latter reaction is sufficiently exothermic that the net reaction, $^{20}Ne + {}^{20}Ne \rightarrow {}^{16}O + {}^{24}Mg$, is exothermic. Clearly, neon burning replenishes some of the ^{16}O depleted during carbon burning.

Oxygen and silicon burning. Once neon burning is complete, the next burning stage is that of oxygen. The dominant reaction is $^{16}O + {}^{16}O \rightarrow {}^{28}Si + {}^{4}He$. This phase clearly depletes the oxygen. After oxygen burning, the star will burn ^{28}Si into ^{56}Fe. The effective reaction is $^{28}Si + {}^{28}Si \rightarrow {}^{56}Ni + \gamma$ followed by decay of ^{56}Ni to ^{56}Fe; however, the burning actually occurs by burning through quasi-equilibrium clusters (e.g., Woosley et al. 1973). Little oxygen is produced in this ^{28}Si burning (e.g., Bodansky et al. 1968).

Stellar explosion. Stars that are able to evolve all the way to silicon burning develop iron cores. At that point, the nuclei are in the state with the highest nuclear binding; hence, any rearrangement of their abundances cannot release energy. This means that the star can no longer burn fuel to maintain its pressure against gravity and the stellar core collapses homologously. The inner core collapses subsonically. Once it attains nuclear matter densities, the collapse halts and the core bounces. The outer core, however, collapses supersonically and therefore does not receive the signal to stop collapsing. It crashes onto the already collapsed inner core. This highly non-adiabatic effect generates a shock wave that propagates out through the outer layers of the star. As the shock passes through the stellar layers, it heats and compresses them. This causes further burning (known as explosive burning). The energy imparted to the outer layers by the shock eventually expels them and injects them into interstellar medium. This dramatic stellar death is known as a supernova. In particular, it is a "core-collapse" supernova since the energy powering the explosion arose from the release of gravitational binding energy in the collapse of the stellar core. For a review, see, for example, Woosley et al. (2002).

The modification of the oxygen isotopes due to explosive burning is largely confined to the inner layers of the star. In particular, explosive oxygen burning will deplete the ^{16}O in the ^{16}O-rich layers and explosive neon burning will enhance the ^{16}O in the ^{20}Ne-rich layers. By the time the shock reaches the ^{12}C-rich and ^{4}He-rich regions, however, the post-shock temperatures and densities do not lead to significant changes in the pre-supernova oxygen abundances.

Analysis of the oxygen yields from massive stars

Armed with an understanding of the nucleosynthesis in the mainline burning stages of stellar evolution, we may now analyze the yields from massive stars—those with masses greater than about ten solar masses. Such stars are able to burn their nuclei all the way to iron. Stars with mass less than about ten solar masses develop cores that are supported by electron degeneracy, which halts their evolution before the advanced nuclear burning stages can occur. For a discussion of degeneracy, see the section on low-mass stars below.

To analyze the yields from massive stars, we consider a single model. While this is only one particular model, its yields are fairly representative of the ejecta from any star more than ten times the mass of the Sun. Chemical evolution models using detailed stellar model yields have long shown that the Galaxy's supply of ^{16}O is dominantly from massive stars (e.g., Tinsley 1980). Because ^{16}O so dominates the oxygen abundance, massive stars are thus nearly the sole contributors to the Galaxy's inventory of this important element even though they compose only a few percent of the stars born in any stellar generation. Massive stars also dominate the galactic production of ^{18}O (e.g., Timmes et al. 1995). Low-mass stars only dominate the galactic synthesis of the low-abundance isotope ^{17}O.

The model presented here is that of Meyer (2005), using the stellar evolution code of The et al. (2000) and El Eid et al. (2004) but with coupled nuclear burning and convection using routines written by Jordan et al. (2005), for a star that began with a mass 25 times greater than that of the Sun. By the end of its life, it had lost 3.4 solar masses of material due to stellar winds. The model ran through silicon burning. The collapse of the core and the explosion of the star were then simulated by numerically increasing the energy in the core of the stellar model. This led to the generation of an outwardly propagating shock wave in the model. Shock propagation and the concomitant explosive burning were tracked with the appropriate computer codes.

The final yields (after stellar explosion) of the isotopes of oxygen relative to their initial abundances are shown in Figure 3. The abscissa is the so-called Lagrangian mass coordinate, M_r. The value of M_r indicates the mass contained within a given spherical shell in the star. For example, $M_r = 0$ is the center of the star. $M_r = M$, where M is the total mass of the star, is the star's surface. $M_r = 10$ solar masses locates a spherical shell that contains 10 solar masses inside. The Lagrangian mass coordinate is convenient because, although the radius of a shell expands or contracts as the star evolves, the mass it contains does not.

As Figure 3 shows, the abundances of the oxygen isotopes vary dramatically inside the stellar ejecta. Particularly noteworthy is the fact that abundances are uniform over certain mass ranges. This indicates mixing within the stellar regions. For example, the abundances of ^{16}O, ^{17}O, and ^{18}O are uniform from M_r ~7.8 to 21.6 solar masses. This represents the outer envelope of the star, which stretches from what was the hydrogen-burning shell to the stellar surface. The strong convection in the envelope prior to the explosion homogenizes the abundances. Similarly, the helium-burning shell in the star extends from about $M_r \approx 5.5$ to 7.3 solar masses.

It is also worth noting that stellar burning proceeds through a sequence of core and shell burning. In particular, a given burning stage commences in the center of the star since the temperature is generally highest there. If the energy release is strong enough, the burning drives convection. This draws fuel in from throughout the convective core. Once the burning is complete, the fuel for that burning stage is exhausted throughout the convective core. The star will then contract until the next burning stage begins. Shell burning occurs when the region outside the formerly convective core contracts and heats to the point that the appropriate nuclear fuel can ignite.

With these preliminaries in mind, we may trace a star's evolution from the oxygen isotopes in the star. It is convenient to consider major zones in the stellar ejecta and use the terminology from Meyer et al. (1995) to label these zones by the most dominant elemental abundances, working our way inward from the surface of the star. The H envelope stretches from $M_r \approx 7.8$ to 21.6 solar masses. As the star evolves past the main sequence phase of its life, convection begins in the envelope and reaches down to matter that had experienced partial burning of hydrogen

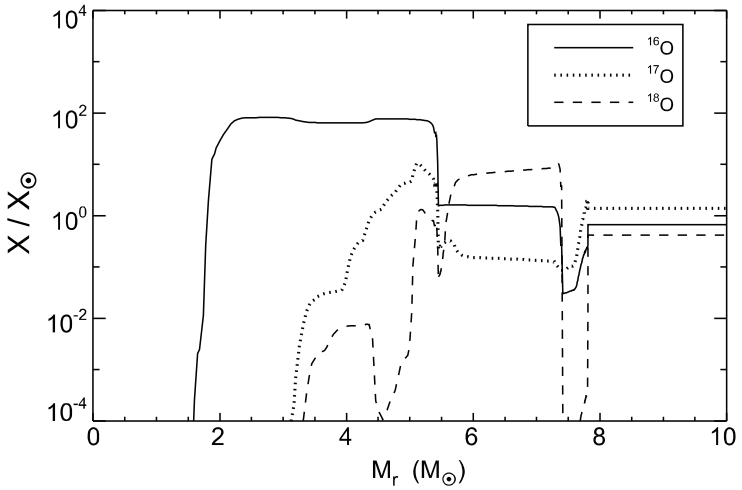

Figure 3. Final mass fractions (after stellar explosion) of the isotopes of oxygen relative to solar in a one-dimensional stellar model of an initially 25 solar mass star as a function of Lagrangian mass coordinate M_r. The final stellar mass was 21.6 solar masses, and the abundances are uniform from $M_r = 7.8$ to 21.6 solar masses (the surface).

by the CNO cycle. As a consequence, the abundances throughout the envelope look similar to the early stages of CNO burning in Figure 1, with modest enrichments in ^{14}N and ^{17}O. It is also noteworthy that mass loss begins as envelope convection commences and carries away some products of CNO burning prior to the explosion.

The He/N zone stretches from $M_r \approx 7.3$ to 7.8 solar masses. It is a thin, radiative (non-convective) shell that was originally part of the convective hydrogen-burning core. Since it largely completed hydrogen burning at the time of stellar explosion, it converted most of its oxygen into ^{14}N, in analogy with the late stages of the single-zone calculation shown in Figure 1, in which all three oxygen isotopes are depleted relative to their initial abundances.

The He/C zone stretches from $M_r \approx 5.5$ to 7.3 solar masses. This is the part of the star that had experienced convective core hydrogen burning and was burning helium in a convective shell at the time of stellar explosion. In this zone, the ^{18}O is enriched, and the abundances resemble those in the single-zone calculation in the early stages of the burning. It is worth emphasizing that, because of the convective burning, a ^{14}N atom that captures a ^{4}He atom in the burning region is likely to mix out into the non-burning parts of the shell before capturing another ^{4}He. This means that the ^{18}O has to cycle back into the burning region before capturing another ^{4}He to become ^{22}Ne, which lengthens the lifetime of the ^{18}O compared to that in the single-zone calculation. This, in turn, explains why the convective helium shell can be enriched in both ^{12}C and ^{18}O, even though Figure 2 might suggest that ^{12}C builds up only after the ^{18}O is declining.

The O/C zone contains material from M_r ~4.5 to 5.5 solar masses. This is matter that was part of the convective helium-burning core but did not partake in convective carbon shell burning. Since this matter completed helium burning, the oxygen here is dominated by ^{16}O. Nevertheless, in this particular stellar model, some ^{17}O and ^{18}O are present due to non-convective burning in this region just prior to the stellar explosion.

The O/Ne zone, ranging from M_r ~3 to 4.5 solar masses, is a region of the star that experienced convective carbon shell burning. As discussed above, at the temperatures of carbon burning, ^{16}O can capture ^{4}He nuclei released by the carbon burning reactions. This thereby depletes the ^{16}O left over from the previous convective core helium burning. As is evident from Figure 3, however, this depletion is fairly slight, and the ^{16}O still strongly dominates the oxygen abundances.

In the present stellar model, the O/Si zone ranges from $M_r \approx 1.8$ to 3 solar masses. This is the region of the star that experienced neon shell burning. As discussed above, the effective neon-burning reaction is $^{20}\text{Ne} + {}^{20}\text{Ne} \rightarrow {}^{24}\text{Mg} + {}^{16}\text{O}$, which increases the ^{16}O abundance slightly.

Finally, inside $M_r \approx 1.8$ solar masses in the present model, the star burns its ^{16}O into ^{28}Si and heavier isotopes both in pre-supernova and supernova nucleosynthesis. These regions of the stellar ejecta, the Si/S and Ni zones, are devoid of any oxygen, except for trace amounts produced during the stellar explosion.

In broad summary, the ejecta from a massive star is characterized by an ^{17}O-rich envelope, which contains most of the stellar ejecta, a narrow helium shell enriched in ^{18}O, and the inner regions, which are strongly enriched in ^{16}O. It is important to emphasize that, although it is true that massive stars can eject several solar masses of ^{16}O, the massive star ejects all three O isotopes, and the bulk ejecta are not necessarily ^{16}O-rich.

Low-mass stars

Apart from mass loss during pre-supernova evolution, which can be significant, massive stars tend to lose all their mass in a single event, namely, the supernova explosion. In contrast, low-mass stars, those with masses less than roughly eight solar masses, lose their mass in periodic episodes during their post-main sequence phases. It is thus necessary to follow the evolution of the star in detail to understand the ejected oxygen yields. We are brief in our

discussion; for more detailed reviews of the evolution of, and mass loss from, low-mass stars, please see Busso et al. (1999), Herwig (2005), or Straniero et al. (2006).

Before discussing the evolution of low-mass stars, it is important to consider the concept of degeneracy in gases. The principal subatomic components of stars are electrons, protons, and neutrons, which all have intrinsic angular momentum quantum number ("spin") ½, which means they are fermions. By the Pauli Exclusion Principle, no two fermions can occupy the same quantum state. This is not a problem at low densities when there are a vastly greater number of states energetically available than electrons present. When the density increases, however, the number of energetically available states does not greatly exceed the number of electrons. This is the condition of degeneracy, and the result is that electrons may find themselves trapped in high-energy states because lower-energy states are already occupied by other electrons. Because these high-energy electrons carry momentum, they contribute significantly to the pressure of the gas. The remarkable consequence is that even a zero-temperature degenerate gas can have a high pressure.

To put this in perspective, consider the pressure at the center of the Sun. The temperature (T) = 1.5×10^7 Kelvins (K) and the mass density is about 150 g/cm^3, which corresponds to a particle density of about $n = 2\times10^{25}$ particles/cm^3 in the fully ionized plasma. This gives rise to a gas pressure $P = nk_BT$ = about 4×10^{16} dynes/cm^2, where k_B is Boltzmann's constant. There are essentially no degenerate electrons in the center of the Sun, so the degeneracy pressure is zero. In the evolved core of a low-mass star, by contrast, the temperature is roughly 10^8 K and the mass density is roughly 10^6 g/cm^3. The gas pressure is thus about $P = 8\times10^{21}$ dynes/cm^2. At the same conditions, however, the degeneracy pressure is about 2×10^{22} dynes/cm^2. The degeneracy pressure dominates that due to the thermal motions of the gas and can be great enough to support the star against contraction due to gravity.

A final introductory point regards burning under degenerate conditions. When nuclear burning occurs, nuclear binding energy is released, which raises the temperature of the local environment. Under non-degenerate conditions, the pressure rises. This causes gas in the local environment to expand, and thus cool. This feedback mechanism can thus lead to steady, stable burning. Under degenerate conditions, however, the pressure is dominated by the degenerate electrons and is thus largely insensitive to the temperature. When burning occurs, the temperature rises but the pressure does not. The rising temperature causes the nuclear burning to proceed at a more rapid rate, which leads to a further increase in temperature and even faster burning. This is a runaway condition that stops only when the temperature is so high that the degeneracy is lifted and the normal gas pressure again dominates. Such violent burning can lead to nova outbursts or to Type Ia supernova explosions (see below).

The typical evolution of a low-mass star begins with core hydrogen burning during main sequence evolution. Once the hydrogen is exhausted, the center of the star contracts, and hydrogen shell burning commences on top of the hydrogen-exhausted core. The star begins to ascend the giant branch in the Hertzsprung-Russell diagram. As the star ascends the giant branch, it grows in radius, and the outer envelope expands and cools. This increases the opacity, and the envelope becomes convective. The convective envelope grows in extent and eventually "dredges up" material that had experienced CNO processing (the "first dredge up"). This enriches the envelope material in ^{17}O and depletes it slightly in ^{16}O and ^{18}O.

The stellar core continues to contract until helium burning ignites. This occurs either under electron-degenerate conditions as a "flash" for stars less than roughly 2 solar masses or under non-degenerate conditions and, hence, more quietly for stars of mass greater than ~2 solar masses. After the core has exhausted its helium, it contracts again and ascends the "asymptotic" giant branch (AGB). At this time, stars more massive than ~4 solar masses experience "second dredge up," which brings products of hydrogen shell and helium core burning to the surface. The CNO burning products tend to dominate so that, again, the ^{17}O is enriched.

By this point, the star's structure consists of an inert, degenerate C/O core, surrounded by a helium-burning shell, surrounded by a hydrogen-burning shell, surrounded by the stellar envelope. The hydrogen- and helium-burning shells burn alternately in a complicated choreography. Most of the time, hydrogen shell burning occurs quiescently. Eventually, however, the temperature and density rise in the helium-rich region between the C/O core and the hydrogen shell. The helium ignites in a thermal pulse, which drives convection within the helium-rich zone and extinguishes the hydrogen-burning shell. The convective envelope reaches down into matter that has experienced helium burning and dredges it up ("third dredge up") to the surface, thereby enriching it in the helium-burning products, including ^{16}O and ^{18}O, as well as ^{17}O from the hydrogen shell. Once the helium burning has ceased, the newly produced carbon and oxygen settle onto the core, and the hydrogen-burning shell reignites.

The thermal pulses help drive the periodic mass loss from the AGB stars. As a typical AGB star progresses through multiple thermal pulses, the C/O ratio in the envelope increases as the helium shell nucleosynthesis and third dredge up tend to preferentially add ^{12}C over ^{16}O. Because the oxygen abundance initially dominated that of carbon, the star began with a C/O abundance ratio less than one. The preferential addition of ^{12}C increases the C/O ratio until it becomes a "carbon" star (C/O > 1). Eventually the pulsations drive off most the star's envelope, and only a degenerate C/O white dwarf star with a thin hydrogen or helium atmosphere is left behind. The thin atmosphere is due to the remnants of the star's original envelope, or possibly to accretion from the interstellar medium. So-called "naked" white dwarf stars that show no surface hydrogen or helium have also been observed (Werner et al. 2004). Naked white dwarf stars have clearly lost their entire envelopes.

In white dwarf stars, degeneracy pressure is sufficient to hold the star up against gravity, even at zero temperature, so these burnt-out cinders slowly radiate and cool with time. It is interesting that, given good estimates of bare white dwarf cooling rates, one may estimate the age of the galactic disk from the populations of white dwarf stars as a function of their luminosity (e.g., Oswalt et al. 1996).

While this picture of stellar evolution is largely successful in explaining surface abundances of low-mass stars, certain observational puzzles present themselves. First, the surface abundance ratio of $^{12}C/^{13}C$ observed for many red-giant branch stars is lower than predicted by the models. This suggests extra mixing below the conventional convective envelope. Such mixing would bring envelope material into the vicinity of the H-burning shell and allow for some nuclear processing, and then transport it back to the surface. This has been termed "cool bottom processing" (Boothroyd et al. 1995). In addition to helping to explain the carbon abundance puzzle in low-mass red-giant branch stars, cool bottom processing can also explain the low $^{18}O/^{16}O$ ratio in certain AGB star atmospheres and presolar oxide grains (Wasserburg et al. 1995; Boothroyd and Sackmann 1999; Nollett et al. 2003) and the carbon and nitrogen isotopic compositions of many presolar SiC grains (Huss et al. 1997; Nollett et al. 2003). Another puzzle is the large surface ^{17}O enrichments in the handful of observations of J type carbon stars which cannot be explained by standard low-mass-star evolution. The answer may lie in so-called "hot bottom burning". In this scenario, the convective envelope of a star with mass greater than ~5 solar masses extends down to the H-burning shell so that the envelope material itself experiences H burning, heavily depleting ^{18}O and enriching ^{17}O at the stellar surface (e.g., Boothroyd et al. 1995; Lattanzio et al. 1997). As we shall see in the section "Oxygen in Presolar Grains," one generally invokes hot bottom burning and cool bottom processing to explain the oxygen isotopic ratios in certain presolar oxide and silicate grains as well as in stellar atmospheres.

For completeness, it is worth noting that stars with masses in the range of ~8-10 solar masses do not develop degenerate C/O cores; they proceed to core carbon burning. They then eject their envelopes in a manner similar to lower mass stars and leave behind O/Ne/Mg white dwarf stars. As we have seen, the pressure in high-mass stars (stars with mass greater than about

ten times that of the Sun) is never dominated by electron degeneracy. These stars therefore proceed all the way through silicon burning.

Novae and Type Ia supernovae

Novae are thermonuclear explosions that occur when material from a binary stellar companion (main sequence or red giant star) is gradually accreted onto a white dwarf. As the density increases in the outer layers of the white dwarf due to ongoing accretion, nuclear reactions begin to occur. Because these reactions take place under degenerate conditions, a relatively brief thermonuclear runaway occurs, resulting in the optical outburst we know as a "nova." A small amount of processed accreted matter and even some underlying white dwarf material is ejected. Then the system settles down to accrete more material until the next nova outburst.

Although there are many uncertainties in nova modeling, there is reasonably good agreement between nova nucleosynthesis calculations and observed elemental abundances in novae. Novae are not believed to be significant contributors to the galactic budget of most elements; however, they are probably an important source of some rare isotopes, including ^{13}C, ^{15}N, and of interest here, ^{17}O. Calculations predict ejecta with ^{17}O/^{16}O ratios 25-2000 times the solar ratio (José et al. 2004). The ejecta are also typically enriched in ^{18}O. Nevertheless, He burning in massive stars is the dominant source of the galactic ^{18}O, and novae contribute only a small fraction to the galactic inventory.

In some white dwarf-stellar companion binary systems, the central density in the accreting white dwarf can build up to such high temperatures that carbon-burning reactions can ignite. Like the nova outburst, such burning occurs under degenerate conditions but, given the higher temperature sensitivity of carbon-burning reactions compared to those of the CNO bi-cycle relevant for novae, this burning is much more violent. The result is the complete thermonuclear disruption of the white dwarf in what is most likely a Type Ia supernova. Because of the high temperatures attained in a Type Ia event, much of the matter reaches nuclear statistical equilibrium, which means that such supernovae are major contributors to the Galaxy's supply of iron-group isotopes. Nuclear statistical equilibrium does not favor oxygen, however, so the inner parts of Type Ia's do not synthesize much oxygen. In the outer layers of Type Ia supernovae for which the burning front is subsonic, considerable ^{16}O can be produced, principally by explosive carbon and neon burning. Nevertheless, given the relative infrequency of Ia events, they probably only contribute at best a few percent to the Galaxy's inventory of oxygen (e.g., Thielemann et al. 1986). Confirmation of this basic picture comes from the fact that very old, low-metallicity stars show O/Fe ratios greater than the solar value (e.g., McWilliam 1997). Such stars formed early from gas that inherited the ejecta from massive stars that lived and died in our Galaxy's first few million years. Massive stars produce a higher ratio of oxygen (^{16}O) to iron than that present in the Solar System, which explains the high O/Fe ratio in low-metallicity stars. Type Ia supernovae, on the other hand, did not start occurring until the first white dwarf stars formed, many tens to hundreds of millions of years after the Galaxy formed. Since Type Ia supernovae produce much iron with little oxygen, their ejecta lowered the O/Fe ratio in the interstellar medium from its high value in the early Galaxy to the solar value by the time of the Sun's birth.

CHEMICAL EVOLUTION OF THE ISOTOPES OF OXYGEN

A fundamental distinction in nucleosynthesis theory is between *primary* and *secondary* isotopes, and this distinction has important consequences for the evolution of the oxygen abundances in the Galaxy. A primary isotope is one that can be produced from a star initially composed only of hydrogen and helium. A secondary isotope is one that can only be made from pre-existing seed nuclei. These pre-existing seed nuclei come from previous generations of stars, hence the name secondary.

The oxygen isotopes provide clear examples of this distinction. ^{16}O is a classic example of a primary isotope. A star composed initially only of the principal products of Big-Bang nucleosynthesis (^{1}H and ^{4}He) could produce ^{16}O. It would do this by converting its initial ^{1}H into ^{4}He via the PP burning chains. When the ^{4}He subsequently burns by the triple-alpha process, the dominant products would be ^{12}C (another primary isotope) and ^{16}O. By contrast, ^{17}O and ^{18}O are both secondary isotopes, because a star initially composed only of ^{1}H and ^{4}He could not form them. ^{17}O is made by proton-capture on ^{16}O. This occurs during hydrogen burning, and a star initially composed only of ^{1}H and ^{4}He would have no ^{16}O during its hydrogen-burning stage to capture a proton. Similarly, ^{18}O traces its origin back to ^{4}He capture by ^{14}N in the early stages of helium burning. As evident from previous discussions, CNO burning converts most of the star's initial C, N, and O isotopes into ^{14}N because of the slowness of the ^{14}N(p,γ)^{15}O reaction. A star composed initially only of ^{1}H and ^{4}He would not have the C, N, or O isotopes necessary to convert into ^{14}N and, hence, would produce no ^{18}O.

Figure 4 demonstrates the primary vs. secondary nature of the oxygen isotopes. Shown are the results from a suite of stellar evolution and nucleosynthesis calculations by Woosley and Weaver (1995) for a range of initial stellar mass and metallicity. In chemical evolution studies, metallicity is an astronomical term that refers to the mass fraction of isotopes heavier than helium. Early astronomical studies of galactic abundances and chemical evolution only distinguished between hydrogen, helium, and everything else, and the respective mass fractions were X (hydrogen), Y (helium), and Z (the "metals"). In the Solar System, the mass fraction of "metals" is $Z_{\odot}$~0.02, with ^{16}O accounting for half of that component.

As Figure 4A shows, massive stars with a metallicity 1/10,000 as large as that in the Solar System eject as much ^{16}O as do stars with solar or even twice solar metallicity. This confirms ^{16}O's status as a primary isotope because it shows that the ^{16}O yield from a star is essentially independent of the star's initial abundance of elements other than hydrogen or helium. The general trend for all metallicities is that the larger the mass of the star, the more ^{16}O it ejects. This reflects the fact that larger stars have larger helium-burning cores; thus, they produce more ^{16}O. The exception to this trend is that some stars in the suite of models with mass greater than 30 times that of the Sun produce less than their lower-mass peers. This is not a nucleosynthetic effect; rather, it is a consequence of the fact that these models experienced significant fallback during their explosion and formed black holes. The black holes swallowed up much of the ^{16}O, which reduced the ejected yield.

Figures 4B and 4C show the corresponding ejected yields from the suite of stellar models for ^{17}O and ^{18}O. From these plots it is clear that the larger the initial metallicity of the star, the greater the production of ^{17}O and ^{18}O. It is also interesting that, for a given initial metallicity, the yield is only weakly sensitive to initial stellar mass. As we previously saw, the ejected ^{17}O and ^{18}O are produced in shell burning. The size of convective hydrogen and helium burning cores is strongly dependent on the stellar mass. By contrast, the sizes of convective hydrogen and helium shells are less dependent on the stellar mass. This explains the weaker dependence of ^{17,18}O on initial stellar mass than that of ^{16}O.

An important caveat is that the rates for the key proton-capture reactions ^{17}O(p,α)^{14}N and ^{17}O(p,γ)^{18}F have been revised since the calculations shown in Figures 4B and 4C were run. In particular, the preferred values for these reaction rates have increased (Blackmon et al. 1995; Angulo et al. 1999). These increases cause greater destruction of ^{17}O during CNO burning, thereby leading to a decrease in the expected yield of ^{17}O from massive stars. In particular, massive star models using the new ^{17}O proton-capture rates typically show nearly ten-fold reductions in the yield of ^{17}O (e.g., Rauscher et al. 2002). This, in turn, suggests that other sites, particularly AGB stars with hot bottom burning and novae play a significant, if not dominant, role in the synthesis of this isotope. Nevertheless, as in the massive star models, the production of ^{17}O is secondary in these other sites (e.g., Romano and Matteucci 2003).

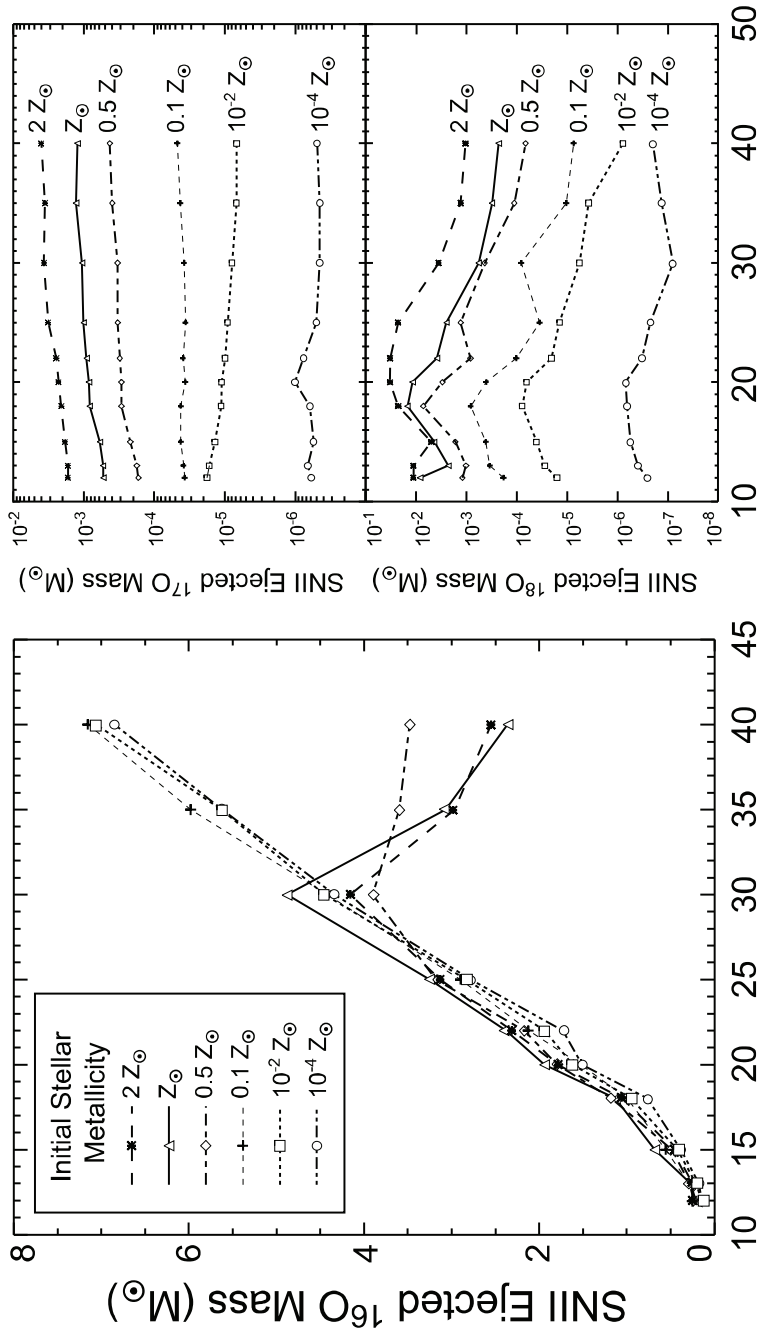

Figure 4. Yields of O isotopes from stellar models of type II supernovae of different initial metallicity and mass, from Woosley and Weaver (1995). This figure was produced by the online Clemson University Galactic Chemical Evolution (CUGCE) Tool available at *http://webnucleo.org*. With this tool, the interested user may explore the primary vs. secondary nature of many other isotopes from massive stars.

With these basics in mind, the galactic evolution of the abundances of the oxygen isotopes is now easy to understand. The high entropy of the Universe allowed primordial nucleosynthesis to produce only ^{1}H, ^{2}H, ^{3}He, ^{4}He, and trace amounts of lithium, beryllium, and boron from the initial soup of neutrons, protons, and electrons. The initial composition of the first generation of stars, then, was devoid of C, N, and O, and as a consequence, produced little ^{17}O and ^{18}O but normal amounts of ^{16}O. As the Galaxy evolved, the succeeding generations of stars formed from interstellar media that had initial compositions enriched in "metals" from previous generations. These stars were then able to produce increasingly large amounts of ^{17}O and ^{18}O.

This behavior is evident in Figure 5, which shows a one-zone model of the evolution of the oxygen abundances in the Galaxy. Like Figure 4, Figure 5 was produced from the online CUGCE Tool at *http://webnucleo.org* (for a description, see Meyer et al. 2001). The model followed a single zone in the Galaxy, used the instantaneous recycling approximation, and employed Clayton's family of analytic galactic infall models (Clayton 1984). Figure 5 shows the mass fraction of oxygen isotopes in the interstellar gas, normalized to their mass fraction at the time of Solar System formation in the model. The behavior of ^{16}O is distinctly different from that of ^{17}O and ^{18}O in the figure. Because ^{16}O is a primary isotope, each generation of stars ejects about the same number of grams of ^{16}O per gram of mass going into stars; thus, the gas becomes enriched in ^{16}O in a linear fashion. In contrast, ^{17}O and ^{18}O are secondary isotopes; therefore, the number of grams of these isotopes ejected per gram going into stars increases with each generation. This gives rise to the quadratic evolution seen in Figure 5. At the time of Solar System formation, the oxygen isotopes had all reached their solar values in the Galaxy.

The galactic chemical evolution presented in Figure 5 is a simplification, given the fact that the model contains only a single zone and uses the instantaneous recycling approximation—the real Galaxy is an inhomogeneous mix of different interstellar phases and stars that have finite lifetimes. Nevertheless, the general trend of increasing ^{17}O and ^{18}O relative to ^{16}O in the evolution

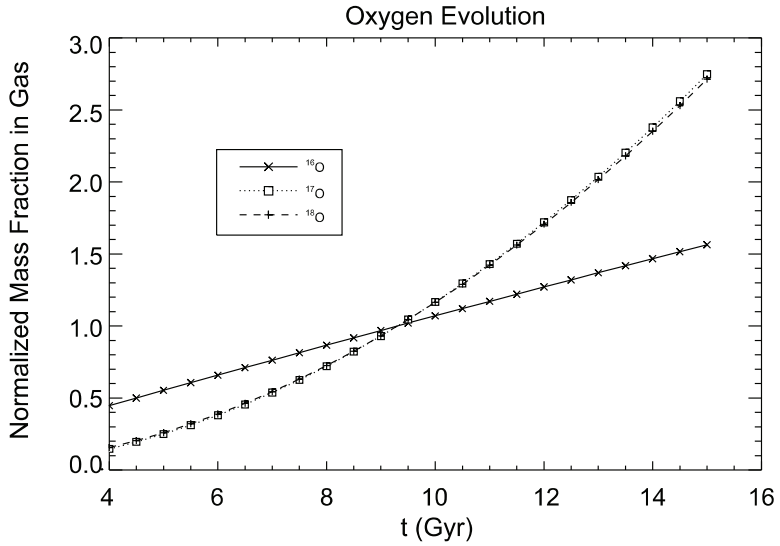

Figure 5. Mass fraction of the isotopes in the interstellar gas in a chemical evolution model as a function of time. The mass fractions are normalized to their values at the time of Solar System formation (roughly 9.5 Ga after Galaxy formation in the present model). On the scale of the plot, t=0 corresponds to the point in time when the Galaxy starts forming. Build up of the mass of the Galaxy occurs over ~2-3 Ga after t=0 by infall of intergalactic gas.

of the Galaxy is quite evident from astronomical data. In particular, stars that formed recently in the local stellar neighborhood show a lower $^{16}O/^{17}O$ ratio than the solar value, which indicates the ratio has declined over the last 4.5 Ga, as expected from galactic chemical evolution (e.g, Wilson and Rood 1994). As for ^{18}O, the $^{16}O/^{18}O$ ratio decreases inward from the Sun's position in the Galaxy. Since the inner part of the Galaxy is thought to be more chemically evolved than the outer regions, this supports a secondary nature of ^{18}O.

Despite this agreement between observations and galactic chemical evolution expectations for oxygen, there are two significant puzzles. The first is that the solar $^{16}O/^{18}O$ ratio is actually less than that in today's interstellar medium in the local solar neighborhood (Wilson and Rood 1994). This is not expected, because the $^{16}O/^{18}O$ ratio in the Galaxy should decline with time. The second puzzle is that the $^{18}O/^{17}O$ ratio in today's interstellar medium is about 3.5, which is significantly less than the solar value of 5.2. From Figure 5, one would expect this ratio to be little changed since the time of the Sun's formation.

A proposed solution to the "^{18}O puzzle" is that the Sun formed in an association of high-mass stars, a so-called "OB association". In such a stellar association, the high-mass stars evolve, explode, and self-enrich the cluster. Since the high-mass stars preferentially eject ^{16}O and ^{18}O, the $^{18}O/^{16}O$ and $^{18}O/^{17}O$ ratios can grow over the course of a ~10-20 Myr period of the association's evolution (e.g., Prantzos et al. 1996). This means that the Sun would have formed with higher values for these ratios than the ambient interstellar medium from which the entire association itself formed.

D. D. Clayton has proposed an alternative scenario. It is based on his idea (Clayton 2003) for origin of the silicon isotopes in presolar silicon carbide grains (see section "Oxygen in Presolar Grains") in which the absorption of a metal-poor satellite galaxy (like the Magellanic Clouds) by the Milky Way initiated a burst of star formation. The number of AGB stars formed during this starburst exceeded that formed by normal galactic star formation, so the former contributed the bulk of the SiC in this period. Since the parent composition of these AGB stars was a mix of the evolved Milky Way Galaxy and the metal-poor satellite, the silicon isotopic compositions of the SiC grains from these stars essentially lie on a mixing line between these two initial compositions. In this scenario, the Sun itself formed with a composition relatively close to the metal-poor satellite; thus, most SiC grains have a silicon isotopic composition that looks more evolved than solar.

This scenario has interesting implications for the ^{18}O puzzle (Clayton 2004). In particular, immediately after the merger, high-mass stars quickly evolved and enriched the interstellar medium with ^{16}O and ^{18}O but not ^{17}O, which had to wait for the low-mass stars to evolve. The Sun formed during this period of enriched ^{16}O and ^{18}O, with an $^{18}O/^{17}O$ ratio of 5.2. Over the course of the last 4.5 Ga, however, low-mass stars formed during the starburst returned their ^{17}O-enriched matter and lowered the interstellar $^{18}O/^{17}O$ ratio to its present value of 3.5. Clayton (2004) points out that a consequence of this scenario would be a correlation between $^{18}O/^{16}O$ and $^{17}O/^{16}O$ and the $^{30}Si/^{28}Si$ in presolar SiC grains. Oxygen and silicon isotopes in presolar silicates from low-mass stars would also be expected to show these correlations. The current presolar silicate data set (see section "Oxygen in Presolar Grains") does not show an unambiguous correlation between Si and O isotopes, but there are some technical difficulties with such measurements (Nguyen et al. 2007). While details of this scenario need to be worked out, it is a nice illustration of oxygen at the nexus of nuclear physics, stellar evolution, galactic astronomy, and presolar grains.

OXYGEN IN PRESOLAR GRAINS

Presolar grains are rare and small (nm to 10 μm) mineral grains recovered from primitive meteorites and interplanetary dust particles (IDPs; <50 μm meteorites collected by aircraft

in Earth's stratosphere). Anomalous noble gas patterns in primitive meteorites led to early speculations that presolar grains might be present in the Solar System (e.g., Black and Pepin 1969), but few researchers were convinced until such grains were successfully isolated in 1987 (Lewis et al. 1987; Bernatowicz et al. 1987; Zinner et al. 1987). The isotopic abundances of many elements in individual presolar grains can be measured to high accuracy with secondary ionization mass spectrometry (SIMS) or resonance ionization mass spectrometry (RIMS), and the highly anomalous results unequivocally show that these objects must have condensed in stellar outflows. For recent reviews, see Clayton and Nittler (2004) and Zinner (2007).

Despite oxygen's prevalence over carbon in the Universe, most presolar grains studied to date are carbonaceous. This does not reflect a paucity of O-rich stardust in the Galaxy or Solar System, especially given the dominance of silicates in the interstellar dust population (Kemper et al. 2004). Rather, it is due to the fact that the O-rich stardust is embedded within an overwhelming background of isotopically normal and mineralogically similar O-rich phases that make up the bulk of meteoritic materials. The first presolar grains recognized were carbides and oxides found in acid-resistant residues of meteorites. Silicates, including presolar ones, were dissolved in the preparation of the residues and thus could not be initially identified. Moreover, preliminary searches for presolar silicates in non-etched samples were unsuccessful due to their fine grain size and the high background. A recently introduced ion microprobe, the Cameca NanoSIMS, and a newly developed imaging system for the Cameca 1270 ion probe have overcome these limitations, now enabling *in situ* searches for presolar grains by sub-μm spatial resolution imaging of the oxygen isotopes. Such techniques led first to the discovery of circumstellar silicate grains in anhydrous interplanetary dust particles (Messenger et al. 2003). This was followed by discovery of presolar silicates in primitive meteorites (Mostefaoui and Hoppe 2004; Nagashima et al. 2004; Nguyen and Zinner 2004). The abundance of presolar silicates is greater than that of any other presolar meteoritic phase, with the possible exception of the highly abundant (but more enigmatic) nanodiamonds (Nguyen et al. 2007).

Oxygen in carbonaceous grains

Of the carbonaceous grains identified to date, the most common types are silicon carbide (SiC), graphite, and nanodiamonds. Oxygen occurs in these grains as a trace element and its isotopic composition has only been measured in graphite grains (Amari et al. 1995). The oxygen in presolar graphite grains of relatively low density is characterized by ^{18}O excesses, which points to formation of these grains in the outflows from massive stars. Moreover, other signatures, especially ^{28}Si enrichments and evidence for condensation of live ^{44}Ti, point to a supernova origin (Nittler et al. 1996). The ^{18}O enrichment is from the helium shell (He/C zone) of the ejecta, whereas the ^{28}Si and ^{44}Ti must have originated from the inner, oxygen-rich, regions of the ejecta, indicating significant and heterogeneous mixing of different mass zones prior to grain formation (Travaglio et al. 1999). The difficulty with this scenario is in mixing the stellar zones without obtaining an overall C/O ratio less than unity. In equilibrium chemistry, when C/O < 1, all carbon is locked up into the tightly bound CO molecule, and graphite and carbides are not predicted to form because O is in excess of C.

A possible solution to the problem of forming graphite and SiC in an oxygen-rich environment is that radioactivity from the supernova may inhibit the build up of CO (Clayton et al. 1999). As carbon atoms associate into carbon chains in this scenario, oxidation is also breaking down these chains. Surprisingly, this destruction allows large carbonaceous dust grains to form, as relatively few carbon nucleation sites survive and grow by absorbing the remaining carbon (Deneault et al. 2006). The chemistry of carbon in the oxygen-rich supernova ejecta is rather complex, especially given the complicated nature of the growing carbon chains and rings, and further studies represent an interesting frontier in supernova physics.

Presolar oxide and silicate grains

A large number of presolar O-bearing grains have now been identified in meteorites and IDPs. There is still limited information on the mineralogy of most identified presolar silicates, but Fe-rich and Fe-poor olivine and pyroxene have been found, as well as several non-stoichiometric (and in some cases amorphous) silicate phases. Identified oxide minerals include presolar grains of Al_2O_3 (both in the crystalline corundum form and in an amorphous form; Stroud et al. 2004), spinel ($MgAl_2O_4$), hibonite ($CaAl_{12}O_{19}$), TiO_2 and Cr-rich spinel. Figure 6 shows the O-isotopic ratios of the different types of presolar O-rich grains. For purposes of discussion, the four grain Groups defined by Nittler et al. (1994, 1997) are indicated as well.

Group 1 grains (making up 64% of all presolar oxides and silicates) are typically strongly enriched in ^{17}O and have normal or modestly depleted ^{18}O, relative to solar materials. This indicates formation of these grains in stellar outflows from red giant stars after first dredge up (and second dredge up for sufficiently massive stars) cycled CNO-processed material to the stellar envelope (see section "Nucleosynthesis of the Isotopes of Oxygen"). The distribution of

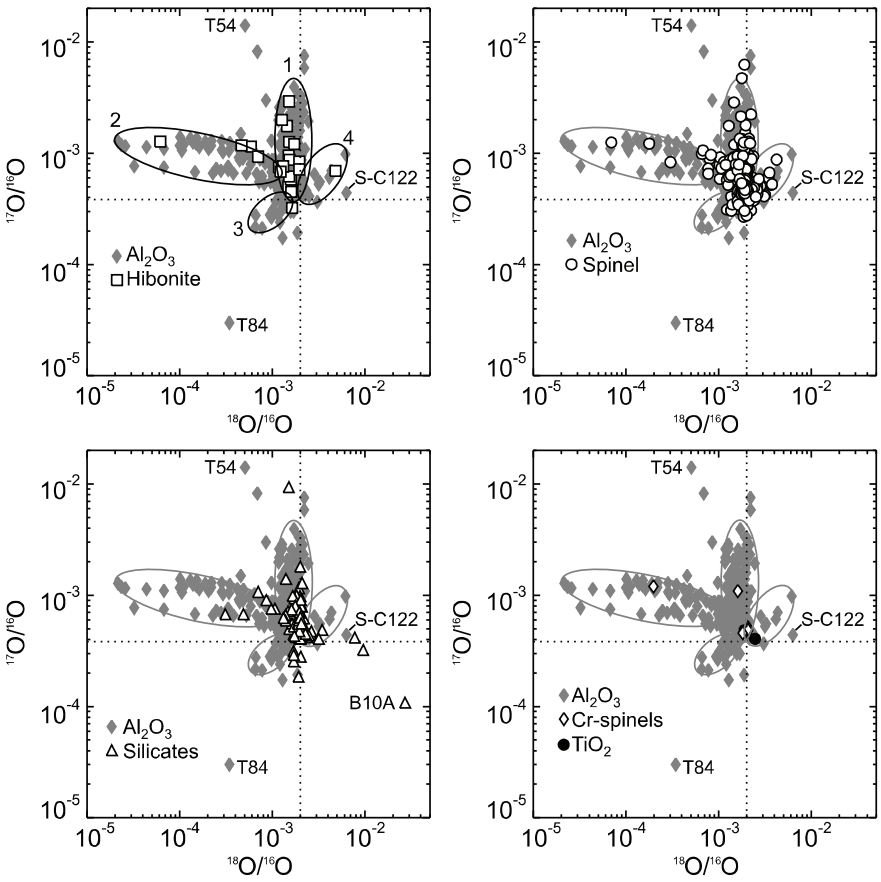

Figure 6. O isotopic ratios of presolar oxides and silicates found in meteorites and interplanetary dust particles. Dotted lines indicate Solar isotopic ratios (assumed to be terrestrial). Ellipses indicate grain Groups defined by Nittler et al. (1994, 1997). Data sources: Huss et al. (1994); Nittler et al. (1994, 1997, 2005a, 2005b); Choi et al. (1998, 1999); Messenger et al. (2003); Zinner et al. (2003, 2005); Mostefaoui et al. (2004); Nguyen et al. (2004); Stadermann et al. (2005).

O isotopes in Group 1 grains are in good agreement with the much less precise observational data for O-rich red giants (e.g., see the comparison in Nittler et al. 1997). Variations in the $^{17}O/^{16}O$ ratio in these grains are thought to be due to variations in the mass of the parent stars. In contrast, variations in $^{18}O/^{16}O$ are too large to be explained by dredge-up models, and probably indicate a range of initial compositions due to galactic chemical evolution (Boothroyd et al. 1994; see section "Chemical Evolution of the Isotopes of Oxygen"). We note that red supergiants are also predicted (and observed, e.g., Harris and Lambert 1984) to have surface ^{17}O enrichments and are thus an alternative source for some Group 1 grains. Assuming that supergiants have $^{17}O/^{16}O$ ratios in the range of $0.9–1.7\times10^{-3}$ (Nittler et al. 1997), we estimate that, at most, about 10-15% of presolar oxides and silicates could have formed in red supergiants. This is in good agreement with many estimates of relative dust production rates of different stars (e.g., Tielens 2005), but not all estimates (Kemper et al. 2004).

Group 2 grains (15% of all grains) show ^{17}O excesses and strong ^{18}O depletions. These isotopic patterns cannot be explained by first or second dredge up—rather, they are best accounted for by extra mixing of material below the base of the standard convective envelope and subsequent "cool bottom CNO processing" (see section "Nucleosynthesis of the Isotopes of Oxygen"). One extreme Group 2 spinel grain most likely originated in an intermediate-mass AGB star undergoing hot bottom burning (Lugaro et al. 2007). Group 3 grains (12% of all grains) are slightly enriched in ^{16}O. It may be that these grains formed in stars of low metallicity since, as we saw in the section "Chemical Evolution of the Isotopes of Oxygen," ^{17}O and ^{18}O are secondary isotopes, and their abundances relative to ^{16}O have been growing with increasing galactic age. Finally, the Group 4 grains (8% of all grains) have moderate ^{17}O and ^{18}O enrichments. Proposed origins of these grains include formation in stars in which third dredge up of early pulse-processed material enriched the envelope ^{18}O composition, formation in stars with higher than solar metallicity, and supernovae.

Some exceptional grains clearly lie outside the four Groups defined by Nittler et al (1994, 1997). A few oxide and silicate grains, the most extreme being Al_2O_3 grain T54, have $^{17}O/^{16}O$ ratios higher than the maximum value of $\sim5\times10^{-3}$ predicted for dredge-up in AGB stars (Boothroyd and Sackmann 1999) as well as normal to moderately depleted ^{18}O abundances. A hot bottom burning origin was previously suggested for grain T54 (Nittler et al. 1997), but this seems unlikely in light of calculations indicating extreme ^{18}O depletions from this process (e.g., Boothroyd et al. 1995; Lugaro et al. 2007). Possibly, grain T54 and the other highly ^{17}O-enriched grains originated in AGB stars, and their compositions indicate a problem with the current dredge-up models (e.g., uncertain reaction rates). Alternatively, these grains have compositions approaching some calculations of nova ejecta, especially novae occurring on low-mass, carbon-oxygen white dwarfs (José et al. 2004). Other outliers from the Groups include a few silicate and Al_2O_3 grains that have ^{17}O depletions but roughly normal $^{18}O/^{16}O$ ratios. These are difficult to understand in terms of dredge-up processes in low- or intermediate-mass stars, since they have $^{17}O/^{18}O$ ratios lower than solar, but the CNO cycles only increase the $^{17}O/^{18}O$ ratio. It is possible that they formed in stars with unusually low initial $^{17}O/^{18}O$ ratios, perhaps due to heterogeneous mixing of supernova ejecta in the interstellar medium (e.g., Lugaro et al. 1999; Nittler 2005).

Of particular interest are Al_2O_3 grain T84, olivine grain B10A, and a few grains with large ^{18}O excesses and close to normal $^{17}O/^{16}O$ ratios (Fig. 6). Although these grains have a wide range of compositions, they all likely formed in Type II supernovae. Grain T84 (Nittler et al. 1998) is extremely enriched in ^{16}O, strongly suggesting an origin in the ^{16}O-rich supernova zones, with little mixing with the ^{18}O-rich and/or ^{17}O-rich outer layers of the ejecta (cf. Fig. 3). Choi et al. (1998) suggested a supernova origin for the ^{18}O-enriched Al_2O_3 grain S-C122. The O composition of this grain and two silicate grains with similar composition (Mostefaoui and Hoppe 2004; Stadermann et al. 2006) can be explained, at least qualitatively, by mixing of

helium-shell (He/C zone, section "Nucleosynthesis of the Isotopes of Oxygen") material with the H envelope, with little or no contribution from the inner ^{16}O-rich zones. One of the ^{18}O-rich silicates also shows an Fe isotope anomaly consistent with a supernova origin (Mostefaoui and Hoppe 2004). Recently, Messenger et al. (2005) have reported the discovery of an olivine grain (B10A) with a very strong enrichment in ^{18}O and a significant depletion in ^{17}O in an IDP. The grain is also modestly enriched in ^{28}Si. This isotopic pattern is reminiscent of that in low-density, presolar graphite grains and similarly suggests a supernova origin. As with the graphite grain compositions, this silicate grain's composition can only be understood if various zones of the supernova ejecta are somehow mixed prior to grain condensation. Moreover, the chemical composition of the grain is that predicted by equilibrium condensation from a gas with composition given by the supernova zone mixture that quantitatively reproduces its isotopic composition. This suggests that despite the extreme conditions present in supernova ejecta, equilibrium thermodynamics might play a role in supernova dust condensation.

The well-preserved structure of B10A also has interesting implications for its transit in the interstellar medium (ISM). The grain has a coating of carbonaceous material. The coating has a ^{15}N excess, which probably signals an origin in a low-temperature molecular cloud environment where chemical reactions give rise to such nitrogen isotopic fractionation. This coating may have protected the grain from the destructive processing that occurs in much of the interstellar medium, which is warm or even hot. On the other hand, the coating's isotopic signature suggests it may not have been present during grain transit from the parent star to the solar nebula. If this is the case, B10A would have to have had a short residence time in the ISM. Messenger et al. (2005) suggest that B10A may have formed in an exploding star from the same molecular cloud in which the Sun formed.

We note that only a small fraction of the presolar oxide and silicate grains apparently originated in supernovae (at most about 9%, if most Group 4 grains are from supernovae). This is consistent with presolar SiC grains, >90% of which are believed to have formed in C-rich AGB stars and only 1% from supernovae. Some recent studies of cold dust in supernova remnants suggest that supernovae are much more prodigious dust producers than previously believed (e.g., Dunne et al. 2003). However, other studies have questioned these results (Dwek 2004; Krause et al. 2004) and the presolar grain evidence indicates that supernovae were relatively minor contributors to dust in the Galaxy at the time that the Solar System formed.

Finally, we note that presolar grains are identified by virtue of having highly anomalous isotopic compositions relative to the range of materials known to have formed in the Solar System. However, this is essentially an operational definition, and analytical uncertainty plays a significant role in deciding whether any given grain is demonstrably a stellar condensate. That is, searches for presolar oxides and/or silicates generally involve the measurement of large numbers of grains, and grains whose isotopic compositions are significantly different (e.g., 3σ) from the rest are defined to be presolar. Figure 7 shows the O-isotopic compositions (expressed as δ-values; see the caption or Criss and Farquhar (2008) for the definition) of many of the presolar grains. Also shown as small ellipses near the origin is the range of O isotopes measured with high precision in meteoritic materials. The grey shaded ellipse illustrates schematically the region of the plot for which analytical uncertainty on small grain measurements has excluded identification of presolar grains. Almost certainly, as analytical methods improve, this region will get smaller and grains with less extreme composition will be defined as presolar. However, it is possible that some presolar grains have isotopic compositions similar to the solar values. One source of such grains may have been other young stars in the molecular cloud from which the Solar System formed. Young stars are observed to eject prodigious amounts of materials in bipolar outflows, and the Sun's stellar neighbors should have had isotopic compositions close to solar values. In any case, we wish to emphasize that establishing the true limits (if any) of presolar grain isotopic compositions is an important topic for future research.

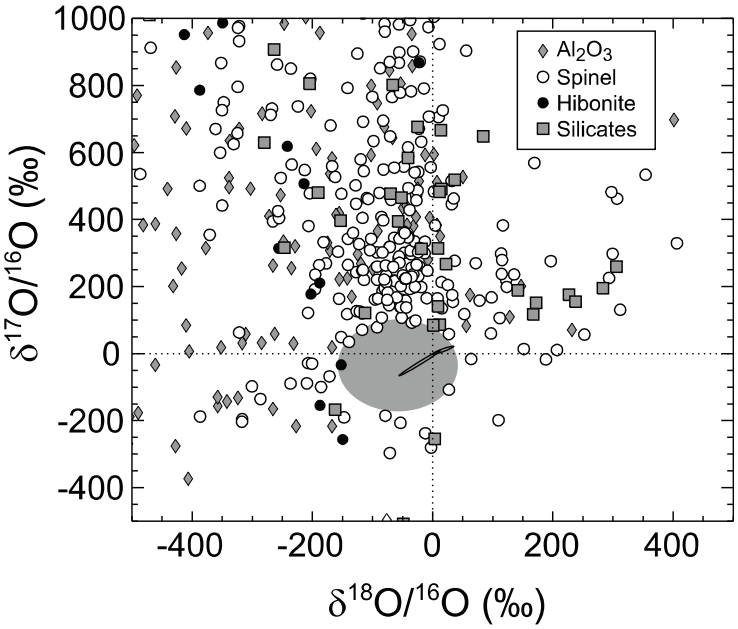

Figure 7. O isotopic ratios of presolar oxides and silicates, expressed as δ-values: $\delta^{i}O = 10^{3}\times[(^{i}O/^{16}O)_{grain}/(^{i}O/^{16}O)_{Terrestrial} - 1\ ]$. Dotted lines indicate solar isotopic ratios (assumed to be terrestrial). Solid ellipses near origin indicate range of high-precision isotopic measurements of Solar System-derived meteoritic materials. Grey shaded ellipse indicates region in which analytical errors preclude identification of presolar grains. See Fig. 6 for data sources.

CONCLUDING REMARKS

We have reviewed in detail the nucleosynthesis and chemical evolution of the O isotopes in the Galaxy. Although the relative abundances of these isotopes are affected by many nuclear processes occurring in many types of stars, it is clear that most ^{16}O and ^{18}O atoms in the Universe were synthesized in massive stars, whereas a major fraction of the ^{17}O probably formed in lower-mass stars and nova ejecta. This basic picture is confirmed by astronomical observations of stars and molecular clouds and by the ability of nucleosynthesis and galactic chemical evolution models to roughly reproduce the composition of the Solar System. Nonetheless, there are significant puzzles, especially the unusual $^{18}O/^{16}O$ ratio of the Solar System, and many important remaining uncertainties in the details of the stellar models. In this regard, presolar grains provide particular promise for improving our understanding of the origin and evolution of O in the Galaxy. Advances in the sensitivity and spatial resolution of isotopic imaging capabilities of SIMS instruments have made it easier to find and study presolar oxides and silicates *in situ,* especially those of submicron size. As we have seen above, such advances have already significantly enhanced our knowledge of stellar evolution by constraining mixing in supernova ejecta and cool bottom processing and hot bottom burning in red giant branch stars. And we anticipate study of oxygen-rich presolar matter will continue to reward us with insights into issues such as chemistry in supernova debris (for example, low-density graphite), chemical evolution (for example, the possible origin of the Group 4 oxide grains), and transit times of dust through the interstellar medium and conditions in the Sun's parent molecular cloud (for example, presolar silicates in IDPs). Such rich rewards are only fitting for oxygen, the king of the strictly stellar synthesized elements.

ACKNOWLEDGMENTS

The authors would like to thank the organizers, particularly Glenn MacPherson, for the stimulating 2005 Oxygen in the Early Solar System workshop in Gatlinburg. BM, LRN and SRM all acknowledge NASA's Cosmochemistry program for financial support of this work.

REFERENCES

Amari S, Zinner E, Lewis RS (1995) Large ^{18}O excesses in interstellar graphite grains from the Murchison meteorite: indication of a massive star origin. Astrophys J 447:L147-L150

Anders E, Grevesse N (1989) Abundances of the elements: meteoritic and solar. Geochim Cosmochim Acta 53:197-214

Angulo C, Arnould M, Rayet M, Descouvemont P, Baye D, Leclercq-Willain C, Coc A, Barhoumi S, Aguer P, Rolfs C, et al. (1999) A compilation of charged-particle induced thermonuclear reaction rates. Nucl Phys A 656:3-183

Bernatowicz T, Fraundorf G, Tang M, Anders E, Wopenka B, Zinner E, Fraundorf P (1987) Evidence for interstellar SiC in the Murray carbonaceous meteorite. Nature 330:728-730

Black, DC, Pepin RO (1969) Trapped neon in meteorites—II. Earth Planet Sci Lett 6:395-405

Blackmon JC, Champagne AE, Hofstee MA, Smith MS, Downing RG, Lamaze GP (1995) Measurement of the $^{17}O(p, {}^4He)^{14}N$ cross section at stellar energies. Phys Rev Lett 74:2642-2645

Bodansky D, Clayton DD, Fowler WA (1968) Nuclear quasi-equilibrium during silicon burning. Astrophys J Supp 16:299-371

Boothroyd AI, Sackmann I-J (1999) The CNO Isotopes: deep circulation in red giants and first and second dredge-up. Astrophys J 510:232-250

Boothroyd AI, Sackmann I-J, Wasserburg GJ (1994) Predictions of oxygen isotope ratios in stars and of oxygen-rich interstellar grains in meteorites. Astrophys J 430:L77-84

Boothroyd AI, Sackmann I-J, Wasserburg GJ (1995) Hot bottom burning in asymptotic giant branch stars and its effect on oxygen isotopic abundances. Astrophys J 442:L21-24

Busso M, Gallino R, Wasserburg GJ (1999) Nucleosynthesis in asymptotic giant branch stars: Relevance for galactic enrichment and solar system formation. Annu Rev Astron Astrophys 37:239-309

Choi B-G, Huss GR, Wasserburg GJ (1998) Presolar corundum and spinel in ordinary chondrites: Origins from AGB stars and a supernova. Science 282:1282-1289

Choi B-G, Wasserburg GJ, Huss GR (1999) Circumstellar hibonite and corundum and nucleosynthesis in asymptotic giant branch stars. Astrophys J 522:L133-136

Clayton DD (1968) Principles of Stellar Evolution and Nucleosynthesis. McGraw-Hill, New York

Clayton DD (1984) Galactic chemical evolution and nucleocosmochronology - Standard model with terminated infall. Astrophys J 285:411-425

Clayton DD (1988) Isotopic anomalies - Chemical memory of Galactic evolution. Astrophys J 334:191-195

Clayton DD (2003) Presolar galactic merger spawned the SiC grain mainstream. Astrophys J 598:313-324

Clayton DD (2004) Solar $^{18}O/^{17}O$ and the setting for solar birth. Lunar Planet Sci XXXV:1045

Clayton DD, Liu W, Dalgarno A (1999) Condensation of carbon in radioactive supernova gas. Science 283:1290-1292

Clayton DD, Nittler LR (2004) Astrophysics with presolar stardust. Annu Rev Astron Astrophys 42:39-78

Criss RE, Farquhar J (2008) Abundance, notation, and fractionation of light stable isotopes. Rev Mineral Geochem 68:15-30

Davis AM, Hashizume K, Chaussidon M, Ireland TR, Prieto CA, Lambert DL (2008) Oxygen in the Sun. Rev Mineral Geochem 68:73-92

Deneault EAN, Clayton DD, Meyer BS (2006) Growth of carbon grains in supernova ejecta. Astrophys J 638:234-240

Dunne L, Eales S, Ivison R, Morgan H, Edmunds M (2003) Type II supernovae as a significant source of interstellar dust. Nature 424:285-287

Dwek E (2004) The detection of cold dust in Cassiopeia A: evidence for the formation of metallic needles in the ejecta. Astrophys J 607:848-854

El Eid MF, Meyer BS, The LS (2004) Evolution of massive stars up to the end of central oxygen burning. Astrophys J 611:452-465

Harris MJ, Lambert DL (1984) Oxygen isotopes in the atmospheres of Betelgeuse and Antares. Astrophys J 281:739-745

Herwig F (2005) Evolution of asymptotic giant branch stars. Annu Rev Astron Astrophys 43:435-479

Huss GR, Fahey AJ, Gallino R, Wasserburg GJ (1994) Oxygen isotopes in circumstellar Al_2O_3 grains from meteorites and stellar nucleosynthesis. Astrophys J 430:L81-84

Huss, GR, Hutcheon ID, Wasserburg GJ (1997) Isotopic systematics of presolar silicon carbide from the Orgueil (CI) chondrite - Implications for solar system formation and stellar nucleosynthesis. Geochim Cosmochim Acta 61:5117-5148

Jordan GC IV, Meyer BS (2004) Nucleosynthesis in fast expansions of high-entropy, proton-rich matter. Astrophys J 617:L131-L134

Jordan GC IV, Meyer BS, D'Azevedo E, Jordan GCI, Meyer BS (2005) Towards in situ calculation of nucleosynthesis in supernova models. Open Issues in Core Collapse Supernova Theory 617:391

José J, Hernanz M, Amari S, Lodders K, Zinner E (2004) The imprint of nova nucleosynthesis in presolar grains. Astrophys J 612:414-428

Kemper F, Vriend WJ, Tielens AGGM (2004) The absence of crystalline silicates in the diffuse interstellar medium. Astrophys J 609:826-837

Krause O, Birkmann SM, Rieke GH, Lemke D, Klaas U, Hines DC, Gordon KD (2004) No cold dust within the supernova remnant Cassiopeia A. Nature 432:596-598

Lattanzio JC, Frost CA, Cannon RC, Wood PR (1997) Hot bottom burning nucleosynthesis in 6 solar mass stellar models. Nucl Phys A 621:435c-438c

Lewis RS, Tang M, Wacker JF, Anders E, Steel E (1987) Interstellar diamonds in meteorites. Nature 326:160-162

Lodders K (2003) Solar system abundances and condensation temperatures of the elements. Astrophys J 591:1220-1247

Lugaro M, Karakas AI, Nittler LR, Alexander CMOD, Hoppe P, Iliadis C, Lattanzio JC (2007) On the asymptotic giant branch star origin of peculiar spinel grain OC2. Astron Astrophys 461:657-664

Lugaro M, Zinner E, Gallino R, Amari S (1999) Si isotopic ratios in mainstream presolar SiC grains revisited. Astrophys J 527:369-394

McWilliam A (1997) Abundance ratios and galactic chemical evolution. Annu Rev Astron Astrophys 35:503-556

Messenger S, Keller LP, Lauretta DS (2005) Supernova olivine from cometary dust. Science 309:737-741

Messenger S, Keller LP, Stadermann FJ, Walker RM, Zinner E (2003) Samples of stars beyond the solar system: Silicate grains in interplanetary dust. Science 300:105-108

Meyer BS (2005) Synthesis of short-lived radioactivities in a massive star. *In*: Chondrites and the Protoplanetary Disk. Krot AN, Scott ERD, Reipurth B (eds) Astronomical Society of the Pacific Conference Series, Vol 34, pp 515-526

Meyer BS, Denny, JE, Clayton DD (2001) Calculating chemical evolution on the Web. Lunar Planet Sci XXXII:1785

Meyer BS, Weaver TA, Woosley SE (1995) Isotope source table for a 25 $M_{\odot}$ supernova. Meteoritics 30:325-334

Mostefaoui S, Hoppe P (2004) Discovery of abundant in situ silicate and spinel grains from red giant stars in a primitive meteorite. Astrophys J 613:L149-L152

Nagashima K, Krot AN, Yurimoto H (2004) Stardust silicates from primitive meteorites. Nature 428:921-924

Nguyen AN, Stadermann FJ, Zinner E, Stroud RM, Alexander CMO'D, Nittler LR (2007) Characterization of presolar silicate and oxide grains in primitive carbonaceous chondrites. Astrophys J 656:1223-1240

Nguyen AN, Zinner E (2004) Discovery of ancient silicate stardust in a meteorite. Science 303:1496-1499

Nittler L (2005) Constraints on heterogeneous galactic chemical evolution from meteoritic stardust. Astrophys J 618:281-296

Nittler L, Alexander CMO'D, Gao X, Walker RM, Zinner E (1994) Interstellar oxide grains from the Tieschitz ordinary chondrite. Nature 370:443-446

Nittler L, Alexander CMO'D, Gao X, Walker RM, Zinner E (1997) Stellar sapphires: The properties and origins of presolar Al_2O_3 in meteorites. Astrophys J 483:475-495

Nittler LR, Alexander CMO'D, Stadermann FJ, Zinner E (2005a) Presolar Al-, Ca-, and Ti-rich oxide grains in the Krymka meteorite. Lunar Planet Sci XXXVI:2200

Nittler LR, Alexander CMO'D, Stadermann FJ, Zinner EK (2005b) Presolar chromite in Orgueil. Meteorit Planet Sci 40:A114

Nittler LR, Alexander CMO'D, Wang J, Gao X (1998) Meteoritic oxide grain from supernova found. Nature 393:222

Nittler LR, Amari S, Zinner E, Woosley SE, Lewis RS (1996) Extinct ^{44}Ti in presolar graphite and SiC: Proof of a supernova origin. Astrophys J 462:L31-34

Nollett K M, Busso M, Wasserburg GJ (2003) Cool bottom processes on the thermally-pulsing AGB and the isotopic composition of circumstellar dust grains. Astrophys J 582:1036-1058

Oswalt TD, Smith JA, Wood MA, Hintzen P (1996) A lower limit of 9.5 Gyr on the age of the Galactic disk from the oldest white dwarf stars. Nature 382:692-694

Prantzos N, Aubert O, Audouze J (1996) Evolution of the carbon and oxygen isotopes in the Galaxy. Astron Astrophys 309:760-774

Rauscher T, Heger A, Hoffman RD, Woosley SE (2002) Nucleosynthesis in massive stars with improved nuclear and stellar physics. Astrophys J 576:323-348
Romano D, Matteucci F (2003) Nova nucleosynthesis and galactic evolution of the CNO isotopes. Mon Not R Astron Soc 342:185-198
Stadermann FJ, Floss C, Bland PA, Vicenzi EP, Rost D (2005) An oxygen-18 rich presolar silicate grain from the Acfer 094 meteorite: A NanoSIMS and ToF-SIMS study. Lunar Planet Sci XXXVI:2004
Straniero O, Gallino R, Cristallo S (2006) s process in low-mass asymptotic giant branch stars. Nucl Phys A 777:311-339
Stroud RM, Nittler LR, Alexander CMO'D (2004) Polymorphism in presolar Al_2O_3 grains from asymptotic giant branch stars. Science 305:1455-1457
The LS, El Eid MF, Meyer BS (2000) A new study of s-process nucleosynthesis in massive stars. Astrophys J 533:998-1015
Thielemann F-K, Nomoto K, Yokoi K (1986) Explosive nucleosynthesis in carbon deflagration models of Type I supernovae. Astron Astrophys 158:17-33
Tielens AGGM (2005) The Physics and Chemistry of the Interstellar Medium. Cambridge University Press, Cambridge
Timmes FX, Woosley SE, Weaver TA (1995) Galactic chemical evolution: hydrogen through zinc. Astrophys J Suppl 98:617-658
Tinsley BM (1980) Evolution of the stars and gas in galaxies. Fund Cosmic Phys 5:287-388
Travaglio C, Gallino R, Amari S, Zinner E, Woosley S, Lewis RS (1999) Low-density graphite grains and mixing in type II supernovae. Astrophys J 510:325-354
Wasserburg GJ, Boothroyd AI, Sackmann I-J (1995) Deep circulation in red giant stars: A solution to the carbon and oxygen isotope puzzles? Astrophys J Lett 447:L37-40
Werner K, Rauch T, Barstow MA, Kruk JW (2004) Chandra and FUSE spectroscopy of the hot bare stellar core H 1504+65. Astron Astrophys 421:1169-1183
Wilson TL, Rood RT (1994) Abundances in the interstellar medium. Annu Rev Astron Astrophys 32:191-226
Woosley SE, Arnett WD, Clayton DD (1973) The explosive burning of oxygen and silicon. Astrophys J 26:231-312
Woosley SE, Heger A, Weaver TA (2002) The evolution and explosion of massive stars. Rev Modern Phys 74:1015-1071
Woosley SE, Weaver TA (1995) The evolution and explosion of massive stars. II. Explosive hydrodynamics and nucleosynthesis. Astrophys J Suppl 101:181-235
Zinner EK (2007) Presolar grains. *In*: Meteorites, Planets, and Comets. Davis AM (ed), Treatise on Geochemistry, Vol 1, 2nd Ed. Holland HD, Turekian KK (ser. eds), Elsevier, Oxford, *http://www.sciencedirect.com/science/referenceworks/9780080437514*
Zinner E, Amari S, Guinness R, Nguyen A, Stadermann FJ, Walker RM, Lewis RS (2003) Presolar spinel grains from the Murray and Murchison carbonaceous chondrites. Geochim Cosmochim Acta 67:5083-5095
Zinner E, Nittler LR, Hoppe P, Gallino R, Straniero O, Alexander CMO'D (2005) Oxygen, magnesium and chromium isotopic ratios of presolar spinel grains. Geochim Cosmochim Acta 69:4149-4165
Zinner E, Tang M, Anders E (1987) Large isotopic anomalies of Si, C, N and noble gases in interstellar silicon carbide from the Murray meteorite. Nature 330:730-732